responses. Characterization of respiratory M cells should accelerate our understanding of the Ag sampling system at work in the upper respiratory tract.

Materials and Methods

Mice

BALB/c mice were purchased from SLC (Shizuoka, Japan). Inhibitor of DNA binding/differentiation 2 $(Id2)^{-/-}$ mice (129/Sv), generated as previously described (11), were maintained together with their littermate $Id2^{+/-}$ mice in a specific pathogen-free environment at the experimental animal facility of the Institute of Medical Science, University of Tokyo. All experiments were carried out according to the guidelines provided by the Animal Care and Use Committees of the University of Tokyo.

M cell staining

For the preparation of nasal cavity samples for confocal microscopy, we decapitated euthanized mice and then, with their heads immobilized, removed the lower jaw together with the tongue. Using the hard palate as a guide, we then used a large scalpel to remove the snout with a transverse cut behind the back molars. After removing the skin and any excess soft tissue, we flushed the external nares with PBS to wash out any blood within the nasal cavity before freezing the nasal passage tissue in Tissue-Tek OCT embedding medium (Miles, Elkhart, IN) in a Tissue-Tek Cryomold. For immunofluorescence staining, we prepared 5-μm–thick frozen sections by using a CryoJane Tape-Transfer System (Instrumedics, St. Louis, MO), allowed the sections to air dry, and then fixed them in acetone at 4°C. We then rehydrated the sections in PBS and incubated them for a further 30 min in Fc blocking solution. For M cell staining, sections were incubated overnight with rhodamine-labeled *Ulex europaeus* agglutinin-1 (UEA-1; Vector Laboratories, Burlingame, CA) at a concentration of 20 μg/ml and FITC-labeled M cell-specific mAb NKM 16-2-4 (12) at 5 μg/ml or FITC-labeled wheat germ agglutinin (WGA; Vector Laboratories, Burlingame, CA) at 10 μg/ml and counterstained with DAPI (Molecular Probes, Eugene, OR) at 0.2 μg/ml in PBS (13).

Electron microscopic analysis of respiratory M cells

For electron microscopic analysis, the nasal cavity sample was prepared and vigorously washed as described above, and then fixed on ice for 1 h in a solution containing 0.5% glutaraldehyde, 4% paraformaldehyde, and 0.1 M sodium phosphate buffer (pH 7.6). After being washed with 4% sucrose in 0.1 M phosphate buffer, the tissues were incubated in an HRP-conjugated UEA-1 solution (20 μg/ml) for 1 h at room temperature. The peroxidase reaction was developed by incubating the tissues for 10 min at room temperature with 0.02% 3,3′-diaminobenzidine tetrahydrochloride in 0.05 M Tris-HCl (pH 8) containing 0.01% H_2O_2. After being washed with the same buffer, the tissues were fixed again with 2.5% glutaraldehyde in 0.1 M phosphate buffer overnight. The nasal passage tissue was decalcified with 2.5% EDTA solution for 5 d. After being washed three times with the same buffer, samples were fixed with 2% osmium tetraoxide on ice for 1 h before being dehydrated with a series of ethanol gradients. For scanning electron microscopy (SEM), dehydrated tissues were freeze-embedded in *t*-butyl alcohol and freeze-dried, then coated with osmium and observed with a Hitachi S-4200 scanning electron microscope (Hitachi, Tokyo, Japan). For transmission electron microscopy (TEM) analysis, the samples were embedded in Epon 812 Resin mixture (TAAB Laboratories Equipment, Berks, U.K.), and ultrathin (70-nm) sections were cut with a Reichert Ultracut N Ultramicrotome (Leica Microsystems, Heidelberg, Germany). Ultrathin sections were stained with 2% uranyl acetate in 70% ethanol for 5 min at room temperature and then in Reynolds lead citrate for 5 min at room temperature. Sections were examined with a Hitachi H-7500 transmission electron microscope (Hitachi, Tokyo, Japan).

Elucidation of M cell numbers

To examine the numbers of respiratory and NALT M cells, mononuclear cells (including M cells, epithelial cells, and lymphocytes) were isolated from the nasal passages and NALT as previously described, with some modifications (4). In brief, the palatine plate containing NALT was removed, and then NALT was dissected out. Nasal passage tissues without NALT were also extracted from the nasal cavity, and mononuclear cells from individual tissues were isolated by gentle teasing using needles through 40-μm nylon mesh. The total numbers of cells isolated from the two preparations were counted. These single-cell preparations were then labeled with PE–UEA-1 (Biogenesis, Poole, England), and the percentages of UEA-1–positive epithelial cells in the nasal passages and NALT were determined with a flow cytometer (FACSCalibur; BD Biosciences, Franklin Lakes, NJ). The numbers of M cells and goblet cells in the nasal passages and NALT were counted by confocal microscopic analysis according to the patterns of staining with UEA-1 and WGA. That is, the frequencies of M cells ($UEA\text{-}1^+WGA^-$) and goblet cells ($UEA\text{-}1^+WGA^+$) were determined by the enumeration of each type in 100 $UEA\text{-}1^+$ cells. The formula used to estimate the number of M cells was: [(total number of mononuclear cells × percentage of $UEA\text{-}1^+$ epithelial cells) × M cells/$UEA\text{-}1^+$ epithelial cells]. The number of respiratory M cells in $Id2^{-/-}$ mice was calculated in the same manner.

Ag uptake in situ

DQ OVA was purchased from Molecular Probes. *Salmonella typhimurium* PhoPc strain transformed with the pKKGFP plasmid was kindly provided by F. Niedergang (14, 15). Group A *Streptococcus* (GAS; *Streptococcus pyogenes* ATCC BAA-1064) was obtained from the American Type Culture Collection (Manassas, VA), and immunofluorescence staining with FITC-conjugated goat anti-*Streptococcus* A Ab (Cortex Biochem, San Leandro, CA) was used to detect GAS uptake. DQ OVA (0.5 mg), GFP-expressing *Salmonella* (GFP-*Salmonella*) (5×10^8 CFU), or GAS (5×10^8 CFU) was intranasally administered and incubated in situ. Thirty minutes after the intranasal administration, the nasal passages were removed as described above and extensively washed with cold PBS with antibiotic solution to remove weakly adherent and/or extracellular DQ OVA or bacteria, as described (13).

The airway fluorescence-labeled Ag-treated nasal passages were processed for confocal microscopy as described above or for FACSCalibur flow cytometric analysis as follows. Mononuclear cells (including M cells, epithelial cells, and lymphocytes) were physically isolated from the nasal passages and NALT as described above, fixed in 4% paraformaldehyde, and labeled with PE–UEA-1 (Biogenesis, Poole, England). The percentage of green fluorescence (BODYPI FL or GFP)/UEA-1 double-positive nasal passage epithelial cells was determined by using an FACSCalibur (BD Biosciences).

To clarify the uptake of the bacteria by M cells, $UEA\text{-}1^+GFP^+$ cells, which were sorted from the nasal passages of mice intranasally infected with GFP-*Salmonella* by using an FACSAria cell sorter (BD Biosciences) were analyzed under three-dimensional confocal microscopy (Leica Microsystems).

To demonstrate the presence of dendritic cells (DCs) in the submucosa of the nasal passages, especially underneath respiratory M cells, after intranasal instillation of GAS, we used FITC- or allophycocyanin-conjugated anti-mouse CD11c (BD Pharmingen, San Jose, CA) Abs for subsequent confocal microscopic analysis.

Immunization

The recombinant *S. typhimurium* BRD 847 strain used in this study was a double *aroA aroD* mutant that expressed the nontoxic, immunogenic 50-kDa ToxC fragment of tetanus toxin from the plasmid pTET*nir*15 under the control of the anaerobically inducible *nirB* promoter (recombinant *Salmonella*-ToxC) (16). As a control, recombinant *Salmonella* that did not express ToxC was used. The recombinant *Salmonella* organisms were resuspended in PBS to a concentration of 2.5×10^{10} CFU/ml. Bacterial suspensions were intranasally administered by pipette (10 μl/mouse) three times at weekly intervals. To eliminate any possible GALT-associated induction of Ag-specific immune responses from the swallowing of bacterial solutions after intranasal immunization, mice were given drinking water containing gentamicin from 1 wk before the immunization to the end of the experiment and were also subjected to intragastric lavage with 500 μl gentamicin solution before and after intranasal immunization. This protocol successfully eliminated the possibility of the intranasally delivered bacteria becoming deposition in the intestine (Supplemental Fig. 1). The titers of tetanus toxoid (TT)-specific serum IgG and mucosal IgA Abs were determined by end-point ELISA, as described previously (17).

To measure GAS-specific immune responses, GAS was suspended in PBS to a concentration of 2×10^{10} CFU/ml. Ten microliters bacterial suspension was intranasally administered once using a pipette. Six weeks after the administration, serum and nasal washes were prepared, and the titers of GAS-specific Ab were measured by ELISA using a previously described protocol (18).

Statistical analysis

Data are expressed as means ± SD, and the difference between groups was assessed by the Mann–Whitney *U* test. The p values <0.05 were considered to be statistically significant.

Results

Respiratory M cells in single-layer epithelium of the nasal passage

The nasal respiratory epithelium of the mouse is composed mainly of pseudostratified ciliated columnar epithelium (19). However, when H&E-stained sections of the whole nasal cavity were examined, a single-layer epithelium was found to cover some regions of the nasal cavity, especially the lateral surfaces of the nasal turbinates (Fig. 1*A–C*). Frozen sections of nasal passages from naive BALB/c mice were prepared and stained with FITC-WGA (green) and rhodamine–UEA-1 (red), and then counterstained with DAPI (blue). Clusters of UEA-1$^+$WGA$^-$ cells that shared M cell characteristics were found exclusively in the single-layer epithelium of the nasal passage covered by ciliated columnar epithelial cells (Fig. 1*D*, 1*E*). Some respiratory M cells were also occasionally found on the transitional area between the single-layer and stratified epithelium. Notably, respiratory M cells also reacted with our previously developed M cell-specific mAb NKM 16-2-4 (12), demonstrating colocalization of the signals of UEA-1 and NKM 16-2-4 (Fig. 1*F*, 1*G*).

Electron microscopic analysis of respiratory M cells

SEM of the respiratory M cells revealed the characteristic features of M cells: a depressed surface with short and irregular microvilli (Fig. 2*A*, 2*B*). TEM analysis revealed that the respiratory M cell was covered by shorter and more irregular microvilli (with definite UEA-1$^+$ signals; Fig. 2*C*, 2*D*) than were found in neighboring ciliated columnar respiratory epithelial cells (Fig. 2*E*). However, no pocket formation (or pocket lymphocytes) was seen in the basal membranes of respiratory M cells, unlike in NALT M cells (Fig. 2*F*, 2*G*). These findings indicated that the newly identified respiratory M cells had most of the unique morphological characteristics of classical M cells.

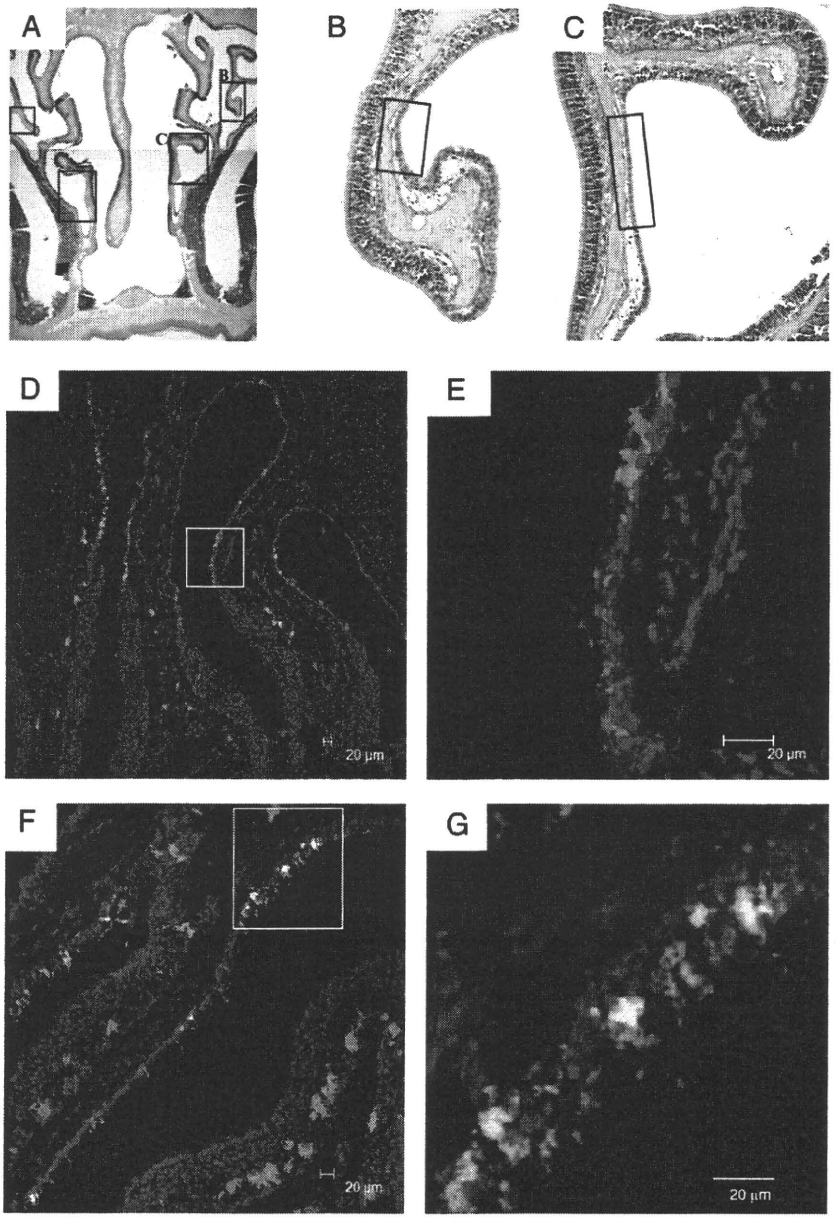

FIGURE 1. Clusters of UEA-1$^+$WGA$^-$ respiratory M cells are found selectively in the single-layer epithelium of the nasal passage. *A–C*, H&E staining reveals the anatomy and general histology of the murine nasal passage (*A*, original magnification ×40). The nasal respiratory epithelium of the mouse is covered with a pseudostratified ciliated columnar epithelium. However, a single-layer epithelium was found on the lateral surfaces of the nasal turbinates (*B*, *C*). Original magnification ×100. Rectangles indicate areas covered with the single-layer epithelium. The results are representative of three independent experiments. *D–G*, Confocal views of UEA-1$^+$ cells in the nasal epithelium of turbinates. Frozen sections were prepared and stained with FITC-WGA (green) and rhodamine–UEA-1 (red), and then counterstained with DAPI (blue) (*D*, *E*). Scale bars, 20 μm. The merged image is shown in *D*. An enlargement of the area in the rectangle in *D* is shown in *E*. UEA-1$^+$WGA$^-$ cells are clustered on the single-layer nasal epithelium of the turbinate. *F* and *G*, UEA-1$^+$ cells also reacted with our previously developed M cell-specific mAb NKM 16-2-4, demonstrating colocalization of signals of rhodamine–UEA-1 (red) and FITC-NKM 16-2-4 (green). The merged image is shown in *F*. An enlargement of an area from the rectangle in *F* is shown in *G*. The results are representative of five independent experiments.

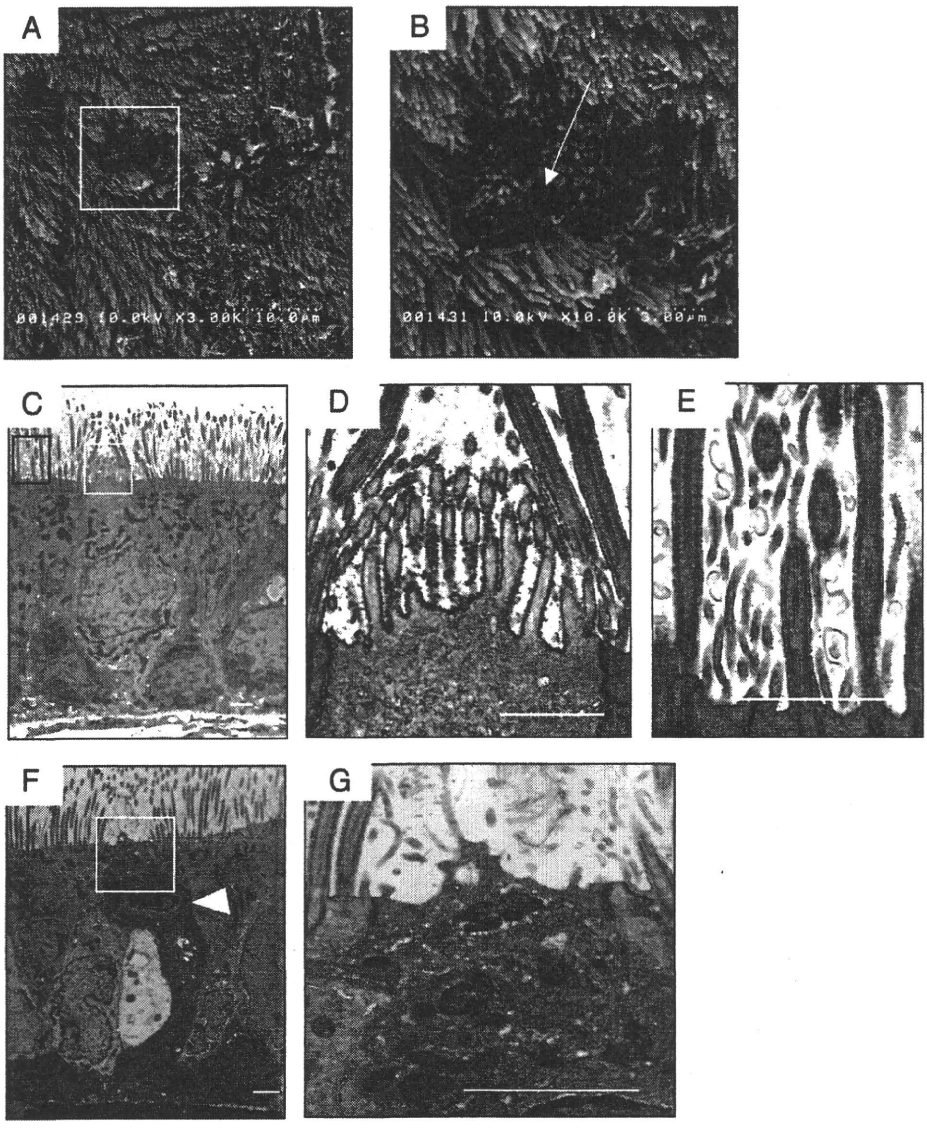

FIGURE 2. Electron microscopic analysis of respiratory M cells. *A* and *B*, SEM analysis shows that the M cells (*B*, arrow) in the nasal passage epithelium are distinguishable from adjacent respiratory epithelial cells by their relatively depressed and dark brush borders. An enlargement of the area in the rectangle in *A* is shown in *B*. As indicated in the *Materials and Methods*, the tissue specimen was incubated with HRP-conjugated UEA-1 before TEM analysis. *C–E*, TEM analysis of respiratory M cells reveals shorter and more irregular microvilli with definite UEA-1$^+$ signals (*D*), unlike the cilia of neighboring respiratory epithelial cells (*E*). *F* and *G*, TEM analysis of NALT M cells. A readily apparent intraepithelial pocket with mononuclear cells (*F*, arrowhead) and short microvilli on the apical surfaces of NALT M cells are seen. The white squares in *C* and *F* indicate UEA-1$^+$ respiratory and NALT M cells, respectively, and are magnified in *D* and *G*, respectively. The black rectangle in *C* indicates an adjacent respiratory epithelial cell and is magnified in *E*. *C–G*, Scale bars, 0.5 μm. Results are representative of four independent experiments.

Protein and bacterial Ag uptake by respiratory M cells

Because M cells were frequently found in the single layer of nasal passage epithelium (Fig. 1*D–G*), we next examined the ability of respiratory M cells to take up various forms of Ag from the lumen of the nasal cavity. DQ OVA or recombinant *Salmonella typhimurium* expressing GFP (*Salmonella*-GFP) was instilled into the nasal cavities of BALB/c mice via the nares. Thirty minutes after the intranasal instillation, immunohistological analyses revealed that the M cells located on the lateral surfaces of the nasal turbinates in the single layer of nasal epithelium had taken up DQ OVA (Fig. 3*A*, 3*B*), as had the M cells located in the NALT epithelium (Fig. 3*C*). Recombinant *Salmonella*-GFP was also observed in M cells in the single layer of nasal epithelium after intranasal administration (Fig. 4*A*, 4*B*). These findings demonstrate that, like NALT M cells (Figs. 3*C*, 4*C*), respiratory M cells were capable of taking up both soluble protein and bacterial Ags.

To further demonstrate the biological significance of respiratory M cells, the numbers of these M cells per mouse were examined and compared with those of NALT M cells (Fig. 3*D*). The number of respiratory M cells was significantly higher than that of NALT M cells. Next, we examined the efficiency of Ag uptake per respiratory M cell and NALT M cell (Figs. 3*E–J*, 4*D–I*). Nasal passage and NALT epithelial cells isolated from BALB/c mice 30 min after intranasal instillation of DQ OVA or recombinant *Salmonella*-GFP were counterstained with PE–UEA-1 for flow cytometric analysis. The UEA-1$^+$ fraction showed a significantly greater efficiency of uptake of DQ OVA Ag and recombinant *Salmonella*-GFP than did UEA-1$^-$ cells isolated from the re-

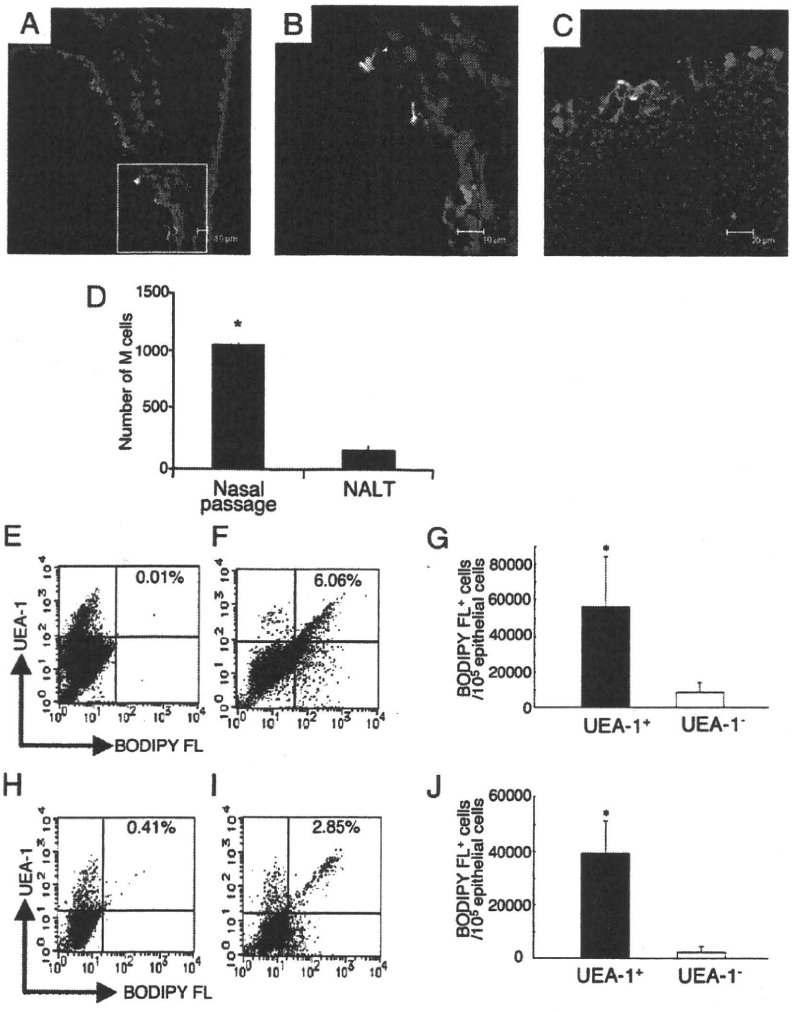

FIGURE 3. Respiratory M cells can take up DQ OVA. *A* and *B*, Immunofluorescence staining of nasal passages in BALB/c mice 30 min after DQ OVA (0.5 mg, green) instillation. Frozen sections of nasal passage were stained with rhodamine–UEA-1 (red) and DAPI (blue). Scale bars, 10 μm. The merged image is shown in *A*. An enlargement of the area in the rectangle in *A* is shown in *B*. These pictures demonstrate DQ OVA uptake by UEA-1$^+$ respiratory M cells. *C*, UEA-1$^+$ (red) NALT M cells in BALB/c mice also show an ability to take up DQ OVA (green). Scale bar, 20 μm. The results are representative of seven independent experiments. *D*, The numbers of UEA-1$^+$WGA$^-$ cells in nasal passages and NALT were quantified. The results are representative of four independent experiments. Flow cytometric analysis of DQ OVA uptake by UEA-1$^+$ respiratory (*E–G*) and NALT (*H–J*) M cells 30 min after intranasal instillation of PBS (*E*, *H*; control) or DQ OVA (*F*, *I*). *G* and *J*, UEA-1$^+$ cells showed significantly higher uptake of DQ OVA than did UEA-1$^-$ cells in the nasal passages and NALT. The results are representative of four independent experiments. $*p < 0.05$.

spiratory epithelium of the nasal passage (Figs. 3*E–G*, 4*D–F*) and NALT (Figs. 3*H–J*, 4*G–I*).

Three-dimensional confocal microscopic analysis demonstrated that UEA-1$^+$ GFP$^+$ cells, which were sorted from the nasal passages of the mice intranasally infected with GFP-*Salmonella*, had captured and taken up the bacteria (Fig. 4*J*, Supplemental Video 1).

Cluster formation by respiratory M cells and DCs in response to inhaled respiratory pathogens

Because respiratory M cells are capable of capturing bacterial Ag, we considered it important to assess these cells as potential new entry sites for respiratory pathogens such as GAS. Confocal microscopic analysis demonstrated that, after its intranasal instillation, GAS stained with FITC–anti-*Streptococcus* A Ab was taken up by UEA-1$^+$ respiratory M cells (Fig. 5*B–E*). SEM analysis also revealed the presence of GAS-like microorganisms on the membranes of respiratory M cells after nasal challenge with GAS (Supplemental Fig. 2*A*). As one might expect, GAS were found in UEA-1$^+$ NALT M cells (Supplemental Fig. 2*B*) as well, confirming a previously reported result (20). Our findings suggest that respiratory M cells act as alternative entry sites for respiratory pathogens.

When we examined the site of invasion by GAS, we noted the presence of CD11c$^+$ DCs underneath the respiratory M cells (Fig. 5). Confocal microscopic analysis of the nasal passage epithelium after intranasal instillation of GAS revealed evidence of the recruitment of DCs, some having contact with the GAS, to the area underneath the respiratory M cells (Fig. 5*B–E*). A few DCs were also observed in the nasal passages of naive mice (Fig. 5*A*); these nasal DCs might preferentially migrate to the area underneath the respiratory M cells to receive Ags from these cells for the initiation of Ag-specific immune responses.

Presence of respiratory M cells in NALT-deficient mice

When we examined the numbers of respiratory M cells in the lymphoid structure-deficient Id2$^{-/-}$ mice (including NALT, NALT-null), the frequency of occurrence of respiratory M cells was comparable to that found in their littermate Id2$^{+/-}$ mice (Fig. 6*A*). This finding suggested that development of respiratory M cells occurred normally under NALT-null or Id2-deficient conditions. Frozen tissue samples were next prepared from NALT-null mice that had received fluorescence-labeled bacteria by intranasal instillation. Immunohistological analysis of these samples revealed the presence of recombinant *Salmonella*-GFP in UEA-1$^+$ cells from the nasal epithelium of Id2$^{-/-}$ mice. GFP-positive bacteria were also located in the subepithelial region of the nasal passages, suggesting that, in the NALT-null mice, some of the nasally deposited bacteria were taken up by respiratory M cells (Fig. 6*B*, 6*C*). Flow cytometric analysis confirmed the uptake of recombinant *Salmonella*-GFP by UEA-1$^+$ M cells, with UEA-1$^+$ cells in the nasal passages of Id2$^{-/-}$ mice showing a significantly higher uptake than UEA-1$^-$ cells (Fig. 6*D–F*).

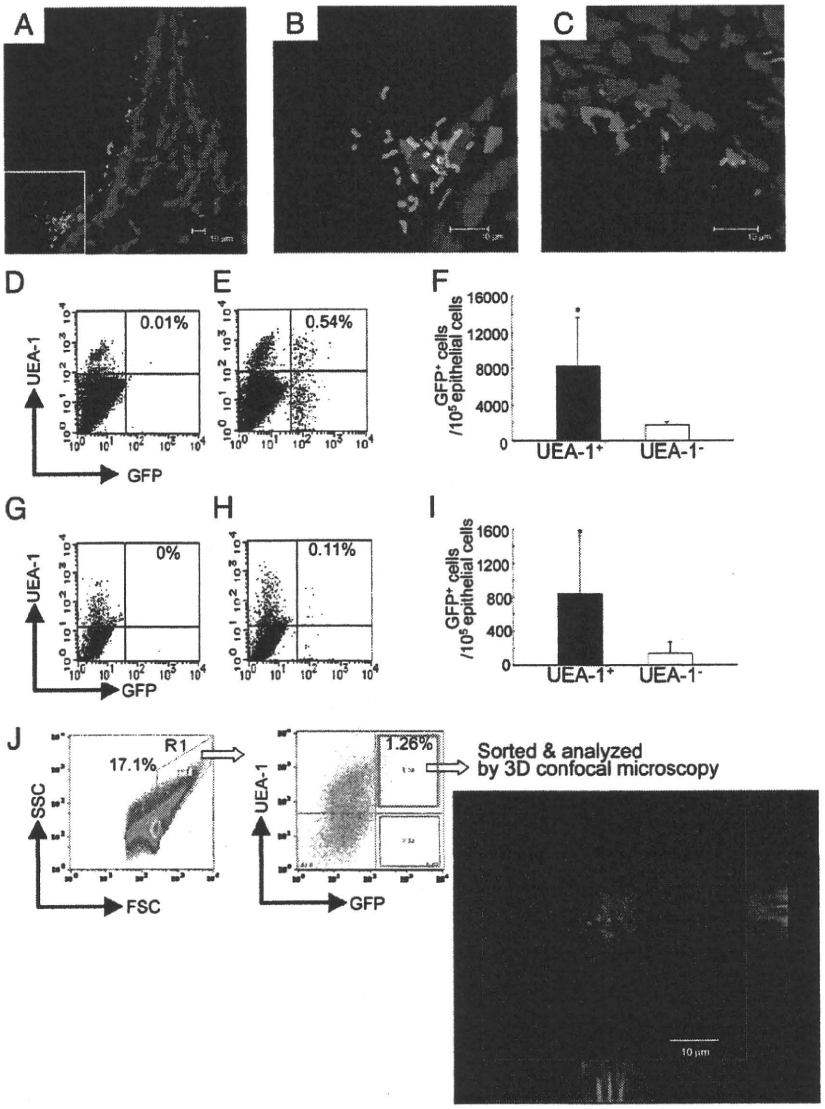

FIGURE 4. Respiratory M cells show an ability to take up recombinant *Salmonella*-GFP. *A* and *B*, Immunofluorescence staining of the nasal passages of BALB/c mice 30 min after GFP-*Salmonella* (5×10^8 CFU, green) instillation. Frozen sections of nasal passage were stained with rhodamine–UEA-1 (red) and DAPI (blue). The merged image is shown in *A*. An enlargement of the area in the rectangle in *A* is shown in *B*. These pictures demonstrate the ability of UEA-1^+ respiratory M cells, like UEA-1^+ NALT M cells (*C*), to take up GFP-*Salmonella*. The results are representative of six separate experiments. *A–C*, Scale bars, 10 μm. Flow cytometric analysis of GFP-*Salmonella* uptake by UEA-1^+ respiratory (*D–F*) and NALT (*G–I*) M cells 30 min after intranasal instillation of PBS (*D*, *G*; control) or GFP-*Salmonella* (*E*, *H*). *F* and *I*, Efficiency of uptake of GFP-*Salmonella* by UEA-1^+ cells in both nasal passages and NALT. The data showed UEA-1^+ M cells to be significantly more efficient than UEA-1^- epithelial cells at taking up GFP-*Salmonella*. The results are representative of five independent experiments. *J*, Three-dimensional confocal microscopic analysis demonstrated that UEA-1^+ GFP^+ cells, which were sorted from the nasal passages of mice intranasally infected with GFP-*Salmonella* (green), took up bacteria. Scale bar, 10 μm. The results are representative of three separate experiments. $^*p < 0.05$.

Induction of Ag-specific immune responses in NALT-deficient mice

NALT-null ($Id2^{-/-}$) mice and their littermate $Id2^{+/-}$ mice were intranasally immunized with recombinant *S. typhimurium* BRD 847 expressing a 50-kDa ToxC fragment of tetanus toxin (recombinant *Salmonella*-ToxC) to examine whether Ag sampling via respiratory M cells could induce Ag-specific immune responses in NALT-deficient mice. To eliminate any possible GALT-associated induction of Ag-specific immune responses from the swallowing of bacterial solutions after intranasal immunization, mice were given drinking water containing gentamicin from 1 wk before the immunization to the end of the experiment and were also subjected to intragastric lavage with 500 μl gentamicin solution before and after intranasal immunization. This protocol successfully eliminated the possibility of the intranasally delivered bacteria becoming deposition in the intestine (Supplemental Fig. 1). The titer of TT-specific serum IgG Ab was as high in $Id2^{-/-}$ mice as in $Id2^{+/-}$ mice (Fig. 6*G*). TT-specific IgA Abs were also detected in the nasal secretions and vaginal washes of intranasally immunized NALT-deficient mice (Fig. 6*H*, 6*I*). As expected, TT-specific Abs were not detected in either $Id2^{-/-}$ or $Id2^{+/-}$ mice intranasally immunized with a control recombinant *Salmonella* that did not express the ToxC gene (Fig. 6*G–I*). In addition to the responses to *Salmonella*, GAS-specific immune responses were induced in the absence of NALT in the experiment with $Id2^{-/-}$ mice (Fig. 6*J–L*). These data indicate that the respiratory M cell is an important Ag-sampling site for the induction of Ag-specific local IgA and serum IgG immune responses.

Discussion

In this study, we show the existence of a novel Ag sampling site for inhaled Ags in the upper respiratory epithelium. The murine nasal membrane has been reported to contain four types of epithelium: respiratory, olfactory, transitional, and squamous (21). Most of the respiratory epithelium is located in the lateral and ventral regions of the nasal cavity and is covered with pseudostratified ciliated columnar cells (21). In this study, we were also able to observe a single-layer epithelium on the lateral surfaces of the turbinates, which was comprised exclusively of UEA-1^+WGA^- M cells (Fig. 1). These respiratory M cells showed specific reactivity to our previously developed M cell-specific mAb NKM 16-2-4 (12). Because NALT is characterized by follicle-associated epithelium, we first thought that this single-layer epithelium could represent the follicle-associated epithelium of the nasal passage. However,

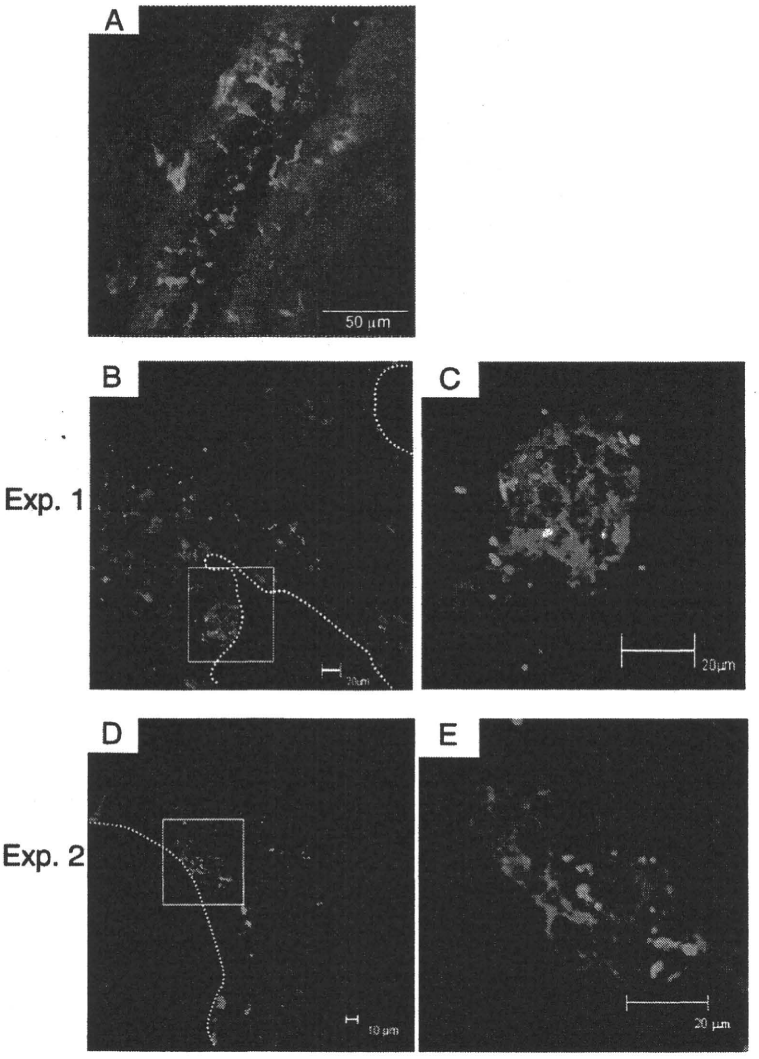

FIGURE 5. Respiratory M cells form clusters with DCs after GAS infection. *A*, Before nasal challenge with GAS, only a few DCs (FITC-CD11c$^+$, green) were associated with UEA-1$^+$ M cells (red) in the nasal passage. Scale bar, 50 μm. *B–E*, Two sets of confocal views of the nasal passage 5 d after intranasal instillation of GAS (Exp. 1 and Exp. 2, respectively). Frozen sections of the nasal passage were stained with FITC–anti-*Streptococcus* A Ab (green), rhodamine–UEA-1 (red), and allophycocyanin-CD11c (blue). These images reveal large numbers of DCs congregated underneath the UEA-1$^+$ respiratory M cells; some of the DCs were closely associated with GAS infiltrated through the UEA-1$^+$ respiratory M cells. *C* and *E* are enlargements of the areas in the squares shown in *B* and *D*, respectively. The results are representative of five independent experiments. *B*, *C*, and *E*, Scale bars, 20 μm; *D*, scale bar, 10 μm.

we ruled out this possibility when we could not find any organized lymphoid structures beneath the single-layer epithelium. The respiratory M cells had most of the classical features of M cells, including a depressed surface covered with short and irregular microvilli. However, TEM analysis revealed that, unlike NALT M cells, they lacked an intraepithelial pocket (Fig. 2). Examination of the numbers of respiratory and NALT M cells per nasal cavity revealed that there were more respiratory M cells than NALT M cells (in general six or seven times more; Fig. 3*D*), suggesting that the respiratory M cell plays a critical role as a gateway for the upper airway.

The anatomical and histological characteristics of the nasal cavity differ markedly between humans and mice. Reflecting this fact, the occurrence of single-layer epithelium also differs between the two species. Murine respiratory epithelium consists of a typical single-layer epithelium with traditional columnar epithelial cells in the turbinate portion of the nasal cavity, whereas pseudostratified columnar epithelium covers the olfactory epithelium (21, 22). In contrast, the traditional single-layer epithelium is not observed in the human nasal cavity, and both the upper respiratory surfaces and the olfactory surfaces are covered by pseudostratified columnar epithelium (23, 24). These differences suggest that the presence of respiratory M cells in the nasal cavity might be a feature unique to the mouse. The presence or absence of respiratory M cells in the human nasal cavity still needs to be carefully examined, and, if these cells are present, their contribution to the uptake of inhaled Ags needs to be investigated in future studies.

Previously, M cells in the lower respiratory tract were found to provide a portal of entry for bacterial pathogens into the lung (25). Our study suggests that the newly identified NALT-independent M cells in the upper respiratory tract provide an alternative portal of entry for nasally inhaled pathogens. The respiratory epithelium comprises three distinct Ag-sampling and/or pathogen-invasion sites: respiratory M cells and NALT M cells in the upper respiratory tract and M cells in the lower respiratory tract. It is interesting to speculate that the nature of the respiratory pathogen may dictate its preferred entry site, with GAS preferentially invading the host via the upper respiratory tract M cells and *Mycobacterium tuberculosis* preferentially invading via the lower respiratory tract M cells. This attractive possibility requires careful examination, and such a line of investigation has been initiated in our laboratory.

Salmonella, a known gastrointestinal pathogen, may have no relevance to the immunological and physiological aspects of Ag uptake by respiratory M cells. However, when used as a live vector for the intranasal delivery of vaccine Ags, attenuated *Salmonella* effectively elicits Ag-specific immune responses (26–29). Pasetti et al. (28) compared intranasal and orogastric immunizations in

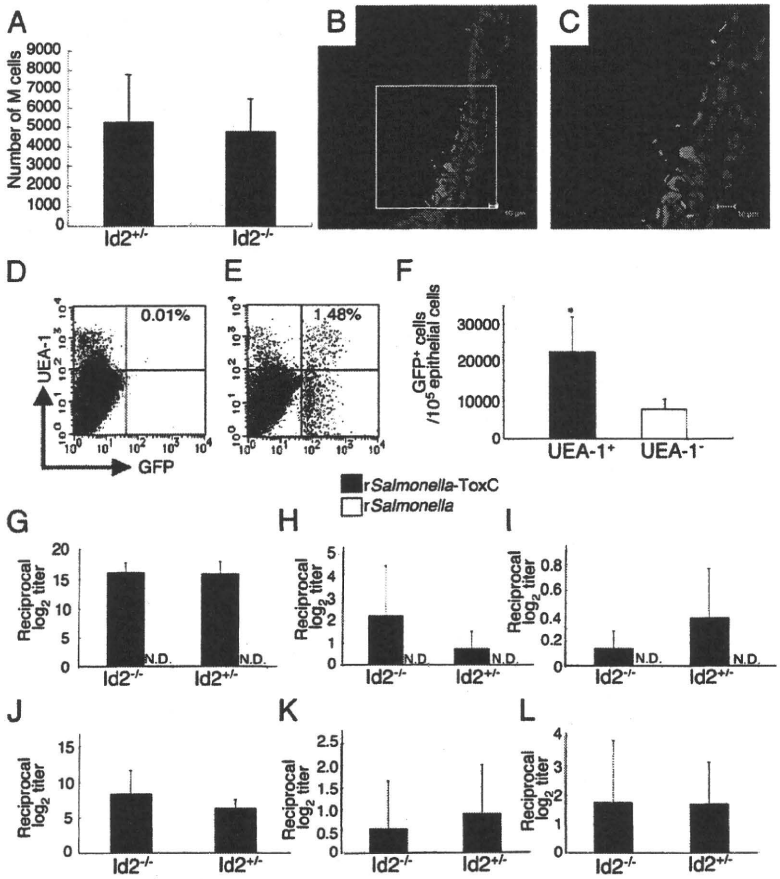

FIGURE 6. Id2$^{-/-}$ mice, which lack NALT, can take up GFP-*Salmonella*, which induce Ag-specific immune responses in UEA-1^{+} respiratory M cells. *A*, The numbers of UEA-1^{+}WGA^{-} cells in nasal passages of Id2$^{-/-}$ and Id2$^{+/-}$ mice were measured. The results are representative of four independent experiments. *B* and *C*, Immunofluorescence staining of nasal passages of Id2$^{-/-}$ mice in which GFP-expressing *Salmonella* (green) had been instilled. Frozen sections of nasal passages were stained with rhodamine–UEA-1 (red) and DAPI (blue). Scale bars, 10 μm. *C* is an enlargement of the area in the square shown in *B*. The results are representative of three independent experiments. *D–F*, Flow cytometric analysis of GFP-*Salmonella* uptake by UEA-1^{+} M cells 30 min after intranasal instillation of PBS (*D*; control) or GFP-*Salmonella* (*E*) in the nasal passages of Id2$^{-/-}$ mice. *F*, Efficiency of uptake by UEA-1^{+} cells in the nasal passages of Id2$^{-/-}$ mice was significantly greater than that by UEA-1^{-} cells. The results are representative of three independent experiments. *G–I*, NALT-deficient (Id2$^{-/-}$) mice and Id2$^{+/-}$ mice were intranasally immunized with recombinant *Salmonella*-ToxC (2.5×10^8 CFU) or recombinant *Salmonella* (2.5×10^8) alone three times at weekly intervals. They were given gentamicin-containing drinking water and also subjected to intragastric lavage with gentamicin solution to eliminate GALT-mediated Ag-specific immune responses. Samples were obtained 7 d after the last intranasal immunization to measure TT-specific Igs by ELISA. Serum IgG (*G*), nasal wash IgA (*H*), vaginal wash IgA (*I*). The results are representative of three independent experiments. *J–L*, As was the case with *Salmonella*, GAS-specific immune responses were induced in the absence of NALT (i.e., in Id2$^{-/-}$ mice), this time by a single intranasal injection of GAS (2×10^8 CFU). Serum IgG (*J*), nasal wash IgA (*K*), vaginal wash IgA (*L*). There were no statistical differences between Id2$^{-/-}$ and Id2$^{+/-}$ mice, as analyzed by the unpaired Mann–Whitney *U* test. The results are representative of five independent experiments. $^{*}p < 0.05$. N.D., not detected.

terms of both Ag-specific immune responses and in vivo distribution of vaccine organisms; they demonstrated that intranasal immunization resulted in greater humoral and cell-mediated immune responses and in the delivery of larger numbers of vaccine organisms to the nasal tissues, lungs, and Peyer's patches. Furthermore, intranasal immunization effectively induces Ag-specific IgA Abs in the reproductive secretions of mice and primates (30, 31). Notably, the levels of Ag-specific IgA Abs in the nasal secretions of NALT-deficient Id2$^{-/-}$ mice were not significantly higher than, or comparable to, those of control tissue-intact mice following intranasal immunization with recombinant *Salmonella* expressing ToxC (Fig. 6*H*) or GAS (Fig. 6*K*), respectively. In contrast, in intranasally immunized NALT-deficient mice, the levels of Ag-specific IgA Abs in remote secretions such as the vaginal wash were not significantly lower than, or comparable to, those in similarly treated tissue-intact mice (Fig. 6*I*, 6*L*). Inasmuch as these results revealed no significant differences between the two groups of intranasally immunized mice, our results at least suggest that respiratory M cells contribute to the induction of Ag-specific immune responses at both local and distant effector sites. However, we still need to carefully examine and compare the contributions of respiratory M cells and NALT M cells in the initiation of Ag-specific IgA Ab responses at local (e.g., airway) and distant (e.g., reproductive tract) effector sites.

In regard to the functional aspects of respiratory M cells, our data demonstrated that the numbers of respiratory M cells that took up OVA were comparable to those of NALT M cells (Fig. 3*G*, 3*J*). In contrast, 10 times more respiratory M cells than NALT M cells took up *Salmonella*; this result suggested that respiratory M cells are more efficient at taking up bacterial (or particulate) Ags than are NALT M cells (Fig. 4*F*, 4*I*). Although we do not have any data regarding the mechanism(s) behind these findings, these results

suggest that there may be functional differences in, for example, Ag uptake capability, between respiratory M cells and NALT M cells due to possible differences in the expression of bacterial Ag receptors, even though the morphologies and phenotypes of these two subsets of M cells are similar. In support of this possibility, it has been shown that the expression of a GP-2–specific receptor for FimH bacteria is restricted to Peyer's patches and not villous M cells; this situation may be analogous to that of NALT and respiratory M cells (32). Although the molecular mechanisms for the induction of Ag-specific immune responses by intranasal immunization and the efficacy of intranasal inoculation await elucidation, we demonstrated in this paper that respiratory M cells, like NALT M cells, are capable of sampling *Salmonella*, thereby opening a new avenue for the uptake of *Salmonella*-delivered vaccine.

CD18-expressing phagocytes (33) and mucosal DCs (34) are involved in the uptake of pathogens from the lumen of the intestine, but their role in the upper respiratory tract has never been clarified. Moreover, we found no evidence that mucosal DCs take up pathogens from the lumen of the nasal passage by expanding their dendrites into the lumen after nasal challenge with GAS. It was recently shown that intranasal immunization of mice with OVA plus adenovirus vector expressing Flt3 ligand as a mucosal adjuvant selectively increases $CD11b^+$ DC numbers in the nasal passages more effectively than those in NALT and subsequently induces Ag-specific Ab and CTL responses (35). Therefore, we speculated that the induction of immune responses in the murine model of intranasal administration of bacteria (e.g., *Salmonella* and GAS) might depend on the presence of appropriate initial Ag sampling sites associated with M cells, which can internalize the vaccine organisms. In this study, DCs were rarely detected in the subepithelial layer or the epithelial layer of the nasal passage in naive mice (Fig. 5*A*). It is important to note that DCs migrated to the area underneath the respiratory M cells and accumulated there to form cell clusters after exposure to respiratory pathogens (Fig. 5*B–D*). Following mucosal exposure to pathogens, submucosal DCs accumulate underneath infected mucosal epithelium that is not associated with organized lymphoid follicles (36, 37). Furthermore, these Ag-capturing DCs are capable of migrating into the draining lymph nodes (dLNs), where they encounter naive T cells for initial Ag-priming (36, 37). The question of whether DCs resident in the nasal passages migrate to the submucosal area to receive inhaled pathogens taken up via respiratory M cells and then travel to the dLNs (e.g., the cervical lymph nodes) to initiate an Ag-specific immune response remains to be addressed. It is interesting to postulate that respiratory M cells could be alternative airway Ag sampling sites for subsequent processing or presentation by nasal passage DCs, thereby initiating Ag-specific immune responses in the dLNs. In support of this hypothesis, it has been shown that Ag-specific Th cells are generated and found in the NALT and dLNs of mice given GAS intranasally (38). Our current study offers proof in support of this hypothesis by showing that *Salmonella* were effectively taken up by upper respiratory tract M cells in NALT and respiratory M cells and that a live vector-containing vaccine Ag induced Ag-specific immune responses via the nasal route.

We showed that TT-specific serum IgG and nasal wash IgA immune responses after intranasal immunization with recombinant *Salmonella*-ToxC were as high in $Id2^{-/-}$ mice as in $Id2^{+/-}$ mice (Fig. 6*G*, 6*H*) and that the frequency of occurrence of respiratory M cells in $Id2^{-/-}$ mice was comparable to that in their littermate $Id2^{+/-}$ mice (Fig. 6*A*). Generally, as discussed above, submucosal and dermal DCs have been shown to migrate to (or to be located in) the area just beneath infected epithelium and to then migrate into the dLNs after they have captured Ags. The DCs then present the peptides derived from these Ags to naive T cells, which subsequently undergo differentiation to Ag-specific effector T cells (36, 37). It has further been suggested that, rather than the DCs harboring Ag-derived peptides migrating to the systemic compartments, such as spleen and other secondary lymphoid tissues, the effector T cells generated in the dLNs after mucosal or vaginal Ag application migrate to these compartments and initiate Ag-specific immune responses (36).

If the cross-talk system between the airway mucosal and systemic immune compartments is similar to that between the reproductive mucosal and systemic immune compartments, it is unlikely that, in $Id2^{-/-}$ mice, the initiation of Ag-specific immune responses, including the presentation of Ags to naive T cells, occurs through migration of nasal DCs into the spleen after the capture of GAS-Ags by respiratory M cells and DCs. However, we cannot rule out this possibility, because it is possible that the nasal immune system, including the system by which Ags are taken up by respiratory M cells, offers distinct Ag-capture, -processing, and -presentation mechanisms via nasal DCs for the generation and migration of Ag-specific effector T cell and B cells. We have also found B-1 cell populations in the nasal passages (N. Tanaka, S. Fukuyama, T. Nagatake, K. Okada, M. Murata, K. Goda, D-Y. Kim, T. Nochi, S. Sato, J. Kunisawa, T. Kaisho, Y. Kurono, and H. Kiyono, manuscript in preparation), and it is possible that these cells may contribute to the induction of Ag-specific Ig responses without any help from $CD4^+$ T cells. At this stage, this is mere speculation, and the precise mechanism needs to be addressed in the future.

Taken together, these findings led us to conclude that respiratory M cells are effective alternative sampling sites for nasally inhaled bacterial Ags and thus play a key role in the induction of systemic and local mucosal immune responses.

Acknowledgments

We thank the staff of the Division of Mucosal Immunology, Institute of Medical Science and the University of Tokyo for technical advice and helpful discussions.

Disclosures

The authors have no financial conflicts of interest.

References

1. Kiyono, H., and S. Fukuyama. 2004. NALT- versus Peyer's-patch-mediated mucosal immunity. *Nat. Rev. Immunol.* 4: 699–710.
2. Yuki, Y., and H. Kiyono. 2003. New generation of mucosal adjuvants for the induction of protective immunity. *Rev. Med. Virol.* 13: 293–310.
3. Fukuyama, S., T. Hiroi, Y. Yokota, P. D. Rennert, M. Yanagita, N. Kinoshita, S. Terawaki, T. Shikina, M. Yamamoto, Y. Kurono, and H. Kiyono. 2002. Initiation of NALT organogenesis is independent of the IL-7R, LTbetaR, and NIK signaling pathways but requires the Id2 gene and CD3(-)CD4(+)CD45(+) cells. *Immunity* 17: 31–40.
4. Hiroi, T., K. Iwatani, H. Iijima, S. Kodama, M. Yanagita, and H. Kiyono. 1998. Nasal immune system: distinctive Th0 and Th1/Th2 type environments in murine nasal-associated lymphoid tissues and nasal passage, respectively. *Eur. J. Immunol.* 28: 3346–3353.
5. Shikina, T., T. Hiroi, K. Iwatani, M. H. Jang, S. Fukuyama, M. Tamura, T. Kubo, H. Ishikawa, and H. Kiyono. 2004. IgA class switch occurs in the organized nasopharynx- and gut-associated lymphoid tissue, but not in the diffuse lamina propria of airways and gut. *J. Immunol.* 172: 6259–6264.
6. Shimoda, M., T. Nakamura, Y. Takahashi, H. Asanuma, S. Tamura, T. Kurata, T. Mizuochi, N. Azuma, C. Kanno, and T. Takemori. 2001. Isotype-specific selection of high affinity memory B cells in nasal-associated lymphoid tissue. *J. Exp. Med.* 194: 1597–1607.
7. Debertin, A. S., T. Tschernig, H. Tönjes, W. J. Kleemann, H. D. Tröger, and R. Pabst. 2003. Nasal-associated lymphoid tissue (NALT): frequency and localization in young children. *Clin. Exp. Immunol.* 134: 503–507.
8. Wiley, J. A., M. P. Tighe, and A. G. Harmsen. 2005. Upper respiratory tract resistance to influenza infection is not prevented by the absence of either nasal-associated lymphoid tissue or cervical lymph nodes. *J. Immunol.* 175: 3186–3196.

9. Lund, F. E., S. Partida-Sánchez, B. O. Lee, K. L. Kusser, L. Hartson, R. J. Hogan, D. L. Woodland, and T. D. Randall. 2002. Lymphotoxin-alpha-deficient mice make delayed, but effective, T and B cell responses to influenza. *J. Immunol.* 169: 5236–5243.
10. Rangel-Moreno, J., J. Moyron-Quiroz, K. Kusser, L. Hartson, H. Nakano, and T. D. Randall. 2005. Role of CXC chemokine ligand 13, CC chemokine ligand (CCL) 19, and CCL21 in the organization and function of nasal-associated lymphoid tissue. *J. Immunol.* 175: 4904–4913.
11. Yokota, Y., A. Mansouri, S. Mori, S. Sugawara, S. Adachi, S. Nishikawa, and P. Gruss. 1999. Development of peripheral lymphoid organs and natural killer cells depends on the helix-loop-helix inhibitor Id2. *Nature* 397: 702–706.
12. Nochi, T., Y. Yuki, A. Matsumura, M. Mejima, K. Terahara, D. Y. Kim, S. Fukuyama, K. Iwatsuki-Horimoto, Y. Kawaoka, T. Kohda, et al. 2007. A novel M cell-specific carbohydrate-targeted mucosal vaccine effectively induces antigen-specific immune responses. *J. Exp. Med.* 204: 2789–2796.
13. Jang, M. H., M. N. Kweon, K. Iwatani, M. Yamamoto, K. Terahara, C. Sasakawa, T. Suzuki, T. Nochi, Y. Yokota, P. D. Rennert, et al. 2004. Intestinal villous M cells: an antigen entry site in the mucosal epithelium. *Proc. Natl. Acad. Sci. USA* 101: 6110–6115.
14. Hopkins, S. A., F. Niedergang, I. E. Corthesy-Theulaz, and J. P. Kraehenbuhl. 2000. A recombinant *Salmonella typhimurium* vaccine strain is taken up and survives within murine Peyer's patch dendritic cells. *Cell. Microbiol.* 2: 59–68.
15. Niedergang, F., J. C. Sirard, C. T. Blanc, and J. P. Kraehenbuhl. 2000. Entry and survival of *Salmonella typhimurium* in dendritic cells and presentation of recombinant antigens do not require macrophage-specific virulence factors. *Proc. Natl. Acad. Sci. USA* 97: 14650–14655.
16. Chatfield, S. N., I. G. Charles, A. J. Makoff, M. D. Oxer, G. Dougan, D. Pickard, D. Slater, and N. F. Fairweather. 1992. Use of the nirB promoter to direct the stable expression of heterologous antigens in *Salmonella* oral vaccine strains: development of a single-dose oral tetanus vaccine. *Biotechnology (N. Y.)* 10: 888–892.
17. Yamamoto, M., P. Rennert, J. R. McGhee, M. N. Kweon, S. Yamamoto, T. Dohi, S. Otake, H. Bluethmann, K. Fujihashi, and H. Kiyono. 2000. Alternate mucosal immune system: organized Peyer's patches are not required for IgA responses in the gastrointestinal tract. *J. Immunol.* 164: 5184–5191.
18. Todome, Y., H. Ohkuni, K. Yokomuro, Y. Kimura, S. Hamada, K. H. Johnston, and J. B. Zabriskie. 1988. Enzyme-linked immunosorbent assay of antibody to group A *Streptococcus*-specific C carbohydrate with trypsin-pronase-treated whole cells as antigen. *J. Clin. Microbiol.* 26: 464–470.
19. Matulionis, D. H., and H. F. Parks. 1973. Ultrastructural morphology of the normal nasal respiratory epithelium of the mouse. *Anat. Rec.* 176: 64–83.
20. Park, H. S., K. P. Francis, J. Yu, and P. P. Cleary. 2003. Membranous cells in nasal-associated lymphoid tissue: a portal of entry for the respiratory mucosal pathogen group A *streptococcus*. *J. Immunol.* 171: 2532–2537.
21. Mery, S., E. A. Gross, D. R. Joyner, M. Godo, and K. T. Morgan. 1994. Nasal diagrams: a tool for recording the distribution of nasal lesions in rats and mice. *Toxicol. Pathol.* 22: 353–372.
22. Adams, D. R. 1972. Olfactory and non-olfactory epithelia in the nasal cavity of the mouse, Peromyscus. *Am. J. Anat.* 133: 37–49.
23. Cagici, C. A., G. Karabay, C. Yilmazer, S. Gencay, and O. Cakmak. 2005. Electron microscopy findings in the nasal mucosa of a patient with stenosis of the nasal vestibule. *Int. J. Pediatr. Otorhinolaryngol.* 69: 399–405.
24. Jafek, B. W., B. Murrow, R. Michaels, D. Restrepo, and M. Linschoten. 2002. Biopsies of human olfactory epithelium. *Chem. Senses* 27: 623–628.
25. Teitelbaum, R., W. Schubert, L. Gunther, Y. Kress, F. Macaluso, J. W. Pollard, D. N. McMurray, and B. R. Bloom. 1999. The M cell as a portal of entry to the lung for the bacterial pathogen *Mycobacterium tuberculosis*. *Immunity* 10: 641–650.
26. Galen, J. E., O. G. Gomez-Duarte, G. A. Losonsky, J. L. Halpern, C. S. Lauderbaugh, S. Kaintuck, M. K. Reymann, and M. M. Levine. 1997. A murine model of intranasal immunization to assess the immunogenicity of attenuated *Salmonella typhi* live vector vaccines in stimulating serum antibody responses to expressed foreign antigens. *Vaccine* 15: 700–708.
27. Locht, C. 2000. Live bacterial vectors for intranasal delivery of protective antigens. *Pharm. Sci. Technol. Today* 3: 121–128.
28. Pasetti, M. F., T. E. Pickett, M. M. Levine, and M. B. Sztein. 2000. A comparison of immunogenicity and in vivo distribution of *Salmonella enterica* serovar *Typhi* and *Typhimurium* live vector vaccines delivered by mucosal routes in the murine model. *Vaccine* 18: 3208–3213.
29. Pasetti, M. F., R. Salerno-Gonçalves, and M. B. Sztein. 2002. *Salmonella enterica* serovar *Typhi* live vector vaccines delivered intranasally elicit regional and systemic specific CD8+ major histocompatibility class I-restricted cytotoxic T lymphocytes. *Infect. Immun.* 70: 4009–4018.
30. Sakaue, G., T. Hiroi, Y. Nakagawa, K. Someya, K. Iwatani, Y. Sawa, H. Takahashi, M. Honda, J. Kunisawa, and H. Kiyono. 2003. HIV mucosal vaccine: nasal immunization with gp160-encapsulated hemagglutinating virus of Japan-liposome induces antigen-specific CTLs and neutralizing antibody responses. *J. Immunol.* 170: 495–502.
31. Imaoka, K., C. J. Miller, M. Kubota, M. B. McChesney, B. Lohman, M. Yamamoto, K. Fujihashi, K. Someya, M. Honda, J. R. McGhee, and H. Kiyono. 1998. Nasal immunization of nonhuman primates with simian immunodeficiency virus p55gag and cholera toxin adjuvant induces Th1/Th2 help for virus-specific immune responses in reproductive tissues. *J. Immunol.* 161: 5952–5958.
32. Hase, K., K. Kawano, T. Nochi, G. S. Pontes, S. Fukuda, M. Ebisawa, K. Kadokura, T. Tobe, Y. Fujimura, S. Kawano, et al. 2009. Uptake through glycoprotein 2 of FimH(+) bacteria by M cells initiates mucosal immune response. *Nature* 462: 226–230.
33. Vazquez-Torres, A., J. Jones-Carson, A. J. Bäumler, S. Falkow, R. Valdivia, W. Brown, M. Le, R. Berggren, W. T. Parks, and F. C. Fang. 1999. Extraintestinal dissemination of *Salmonella* by CD18-expressing phagocytes. *Nature* 401: 804–808.
34. Rescigno, M., M. Urbano, B. Valzasina, M. Francolini, G. Rotta, R. Bonasio, F. Granucci, J. P. Kraehenbuhl, and P. Ricciardi-Castagnoli. 2001. Dendritic cells express tight junction proteins and penetrate gut epithelial monolayers to sample bacteria. *Nat. Immunol.* 2: 361–367.
35. Sekine, S., K. Kataoka, Y. Fukuyama, Y. Adachi, J. Davydova, M. Yamamoto, R. Kobayashi, K. Fujihashi, H. Suzuki, D. T. Curiel, et al. 2008. A novel adenovirus expressing Flt3 ligand enhances mucosal immunity by inducing mature nasopharyngeal-associated lymphoreticular tissue dendritic cell migration. *J. Immunol.* 180: 8126–8134.
36. Zhao, X., E. Deak, K. Soderberg, M. Linehan, D. Spezzano, J. Zhu, D. M. Knipe, and A. Iwasaki. 2003. Vaginal submucosal dendritic cells, but not Langerhans cells, induce protective Th1 responses to herpes simplex virus-2. *J. Exp. Med.* 197: 153–162.
37. Allan, R. S., C. M. Smith, G. T. Belz, A. L. van Lint, L. M. Wakim, W. R. Heath, and F. R. Carbone. 2003. Epidermal viral immunity induced by CD8α^+ dendritic cells but not by Langerhans cells. *Science* 301: 1925–1928.
38. Park, H. S., M. Costalonga, R. L. Reinhardt, P. E. Dombek, M. K. Jenkins, and P. P. Cleary. 2004. Primary induction of CD4 T cell responses in nasal associated lymphoid tissue during group A streptococcal infection. *Eur. J. Immunol.* 34: 2843–2853.